Kim and Cho *Journal of Analytical Science and Technology* (2020) 11:9
https://doi.org/10.1186/s40543-020-00207-9

Journal of Analytical Science and Technology

TECHNICAL NOTE

Improvement of $^{40}Ar/^{39}Ar$ age determinations for Quaternary basaltic rocks by eliminating the peak suppression effect

Jeongmin Kim* and In-Hwa Cho

Abstract

Background: The peak suppression effect, which suppresses the argon isotope signal due to the incomplete cleaning of gas from geological samples during measurement, is found in volatile-rich samples using the ARGUS VI noble gas mass spectrometer and its sample preparation system. Such effect hampers getting the precise isotope ratio essential for the $^{40}Ar/^{39}Ar$ age calculation.

Findings: The addition of one hot-getter and three room-temperature getters to the sample preparation system can effectively eliminate the peak suppression effect for several milligrams of sample during argon measurement to yield highly plausible $^{40}Ar/^{39}Ar$ ages of Quaternary volcanic rocks.

Conclusions: The modified preparation system makes it possible to get highly precise zero-time isotope signals, and thereby a geologically plausible $^{40}Ar/^{39}Ar$ age, especially for a small amount of volatile-rich samples.

Keywords: $^{40}Ar/^{39}Ar$ age, Noble gas mass spectrometer, Quaternary, Peak suppression, Getters

Introduction

The introduction of third-generation noble gas mass spectrometers makes it possible to get a precise $^{40}Ar/^{39}Ar$ age determination for a single grain with the aid of multiple collectors and a laser heating device. Since the installation of the Argus VI noble gas mass spectrometer at the Korea Basic Science Institute (KBSI), many important geological ages have been reported (e.g., Kim et al. 2014). However, for volatile-bearing samples, e.g., volcanic rocks, sulfur-bearing minerals, micas, and amphiboles, precise isotope ratio measurements have been challenging under the original gas preparation system due to the abnormal behavior of argon isotopes (^{40}Ar and ^{36}Ar) during data acquisition. The current $^{40}Ar/^{39}Ar$ dating system has been used to measure small quantities of sample ranging from single grains to several tens of grains weighing less than several milligrams using a laser heating device. In general, as the gas introduced to mass spectrometer is consumed by the ionization in the ion source (McDougall and Harrison 1999), the signal intensities of ^{40}Ar and ^{36}Ar are supposed to decrease during the measurement (Fig. 1). For samples with a very small argon content, the reverse trend is found. Due to such different fractionation of each isotope in the mass spectrometer, zero-time intensities of argon isotopes should be used to calculate the $^{40}Ar/^{39}Ar$ age of samples.

Nevertheless, volatile-rich samples show reverse trends (Fig. 2), that is, the intensities of ^{40}Ar and ^{36}Ar increase during the measurement, in spite of relatively large amounts of argon such as ^{40}Ar > 100 fAmp. Such a weak signal at the beginning of the analysis might be due to the suppression of ionization by the residual volatile component from the samples (Alan Deino, pers. comm.) in the ion source. As measurement progresses, the residual components are gradually removed through ionization in the source chamber and the Ar signal recovers to its normal intensity showing a concave upward signal change. Under these circumstances, it is very difficult to decipher

* Correspondence: j-mkim@kbsi.re.kr
Division of Earth and Environment Science, Korea Basic Science Institute, 162 Yeongudanji-ro, Ochang-eup, Cheongwon-gun, Chungcheongbuk-do 28119, Korea

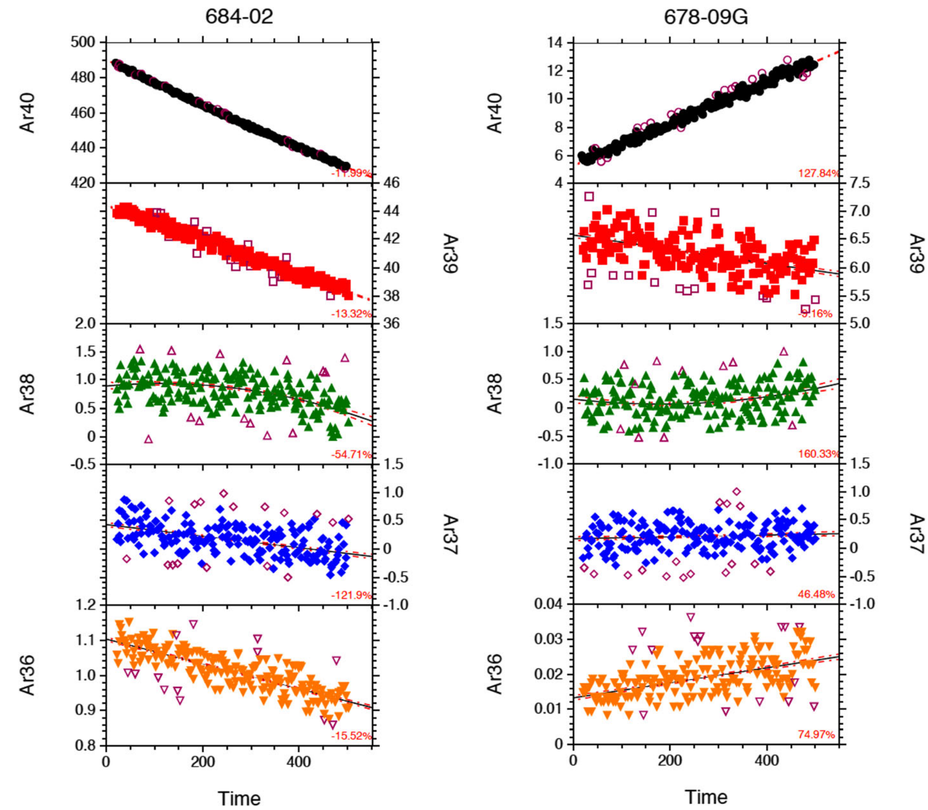

Fig. 1 Normal behavior of Ar isotopes during measurement. All isotope signals are expected to decrease (left) due to the ionization by electron bombardment in the ion source chamber. For samples with small Ar contents (right), the increasing trends are prominent. The red numbers represent the variation of each isotope signal at the beginning and end of the analysis

the plausible zero-time signal for age calculation. Figure 3 shows the age spectrum for the same samples as in Fig. 2. The inconsistent plateau ages and non-uniform age spectrum of each sample aliquot are due to the abnormal signal variation during the measurement.

In this note, we report a procedure to reduce the peak suppression effect under the current configuration of the Argus VI without any significant modification of system hardware. Additionally, the results of age calculations are compared to show the effectiveness of the new protocols in eliminating the peak suppression effect. As an example, the ages of Quaternary volcanic rocks from the Jeongok area in central Korea are presented with their geological significance.

Consequences of the peak suppression effect

$^{40}Ar/^{39}Ar$ age calculations are based on the measured $^{40}Ar/^{39}Ar$ ratio which is proportional to $^{40}Ar/^{40}K$ of sample. Other Ar isotope ratios (e.g., $^{36}Ar/^{40}Ar$ and $^{37}Ar/^{40}Ar$) need to be measured to correct the effect of air-derived and reactor-induced argon (e.g., Kim and Jeon 2015). So the precise measurement of each isotope is essential to obtain a reliable $^{40}Ar/^{39}Ar$ age. As mentioned earlier, under the original configuration of the gas preparation system, the zero-time intensities of ^{40}Ar and ^{36}Ar are severely distorted for volatile-rich samples. Table 1 shows the unreliable age results based on the distorted zero-time isotope ratio. Uncertainties for individual analyses in the data tables are at a 1σ level. Sample SS06-2 (run ID 564) is basaltic rock from Jeju Island in Korea and its eruption age is assumed to be less than 500 Ka. As an example, aliquot 564-06 shows an increasing ^{40}Ar signal (Fig. 2) with unreliable zero-time ^{40}Ar intensity of 67 fAmp during measurement. The age probability diagram of each aliquot (Fig. 4), as well as the spectrum diagrams (Fig. 3), shows a very scattered pattern with a mean age of 430 ± 200 Ka (MSWD = 8), which is inconsistent with the volcanostratigraphic evidence.

As another example, the result for alunite (run ID 427) is presented in Table 2. As a sulfur-bearing mineral ($(K,Na)Al_3(SO_4)_2(OH)_6$), it also shows the increasing ^{40}Ar signal during measurement (Fig. 2). Ages of each aliquot are so scattered (Fig. 5) that the mean age of 5.02 ± 2.0 Ma (MSWD = 18) is geologically meaningless.

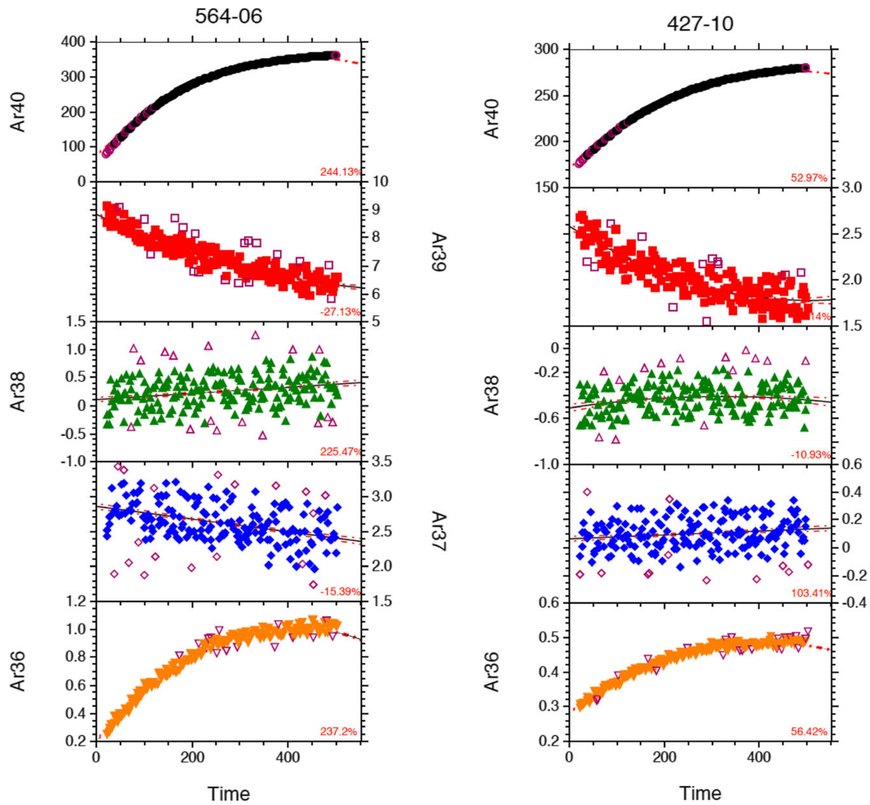

Fig. 2 Examples of the peak suppression effect in ^{40}Ar and ^{36}Ar signals for volatile-rich samples: (left) basaltic rock, (right) alunite. Note that the ^{40}Ar and ^{36}Ar signals gradually increased during the measurement, so that it is not possible to deduce meaningful zero-time signals

Modification of the gas cleaning protocol

The ^{40}Ar/^{39}Ar age dating system at KBSI can be divided into the following three parts: (1) laser heating system, (2) gas preparation bench and (3) high-sensitivity noble gas mass spectrometer. The original configuration of the gas preparation system is shown in Fig. 6a. In order to purify argon from the extracted gases, three SORB-AC getter pumps have been used. They are constructed from a cartridge of getter material (ST101 alloy of zirconium with 16% aluminum) placed around an axial heater. At room temperature, these getters pump out hydrogen and carbon monoxide which are major background gases in the mass spectrometer. The getter can be run at 400 °C to enhance the pumping of less reactive gases such as hydrocarbons. The vacuum level in the gas preparation system reaches $\sim 2 \times 10^{-9}$ mbar by ion pump. Standard air (0.1 cm^3) from the automatic pipette system consisting of a standard volume and two pneumatic valves is routinely measured to derive the discrimination factor.

To reduce the peak suppression effects, various cleaning protocols were tested, e.g., an extension of cleaning time, increasing the number of getters, and the adoption of a water-cooled hot getter. Of these, it was the operation of one hot getter with three room-temperature getters that was the most effective. For this configuration, 40 V of AC was supplied to the internal heater in one of the getters and its external housing was cooled by water to reduce the emanation of particles from the internal surface. Figure 6b shows the modified gas preparation system. It would be best to attach a cooling device to the cold trap shown in Fig. 6 to remove water from the sample, but under current circumstances, this protocol is the next best way to reduce the peak suppression effect described above.

Results

Using the modified configuration, the peak suppression effect is significantly reduced so that the Ar isotope beam intensity decreases to show normal behavior. Figure 7 and Tables 3 and 4 show the behavior of each isotope and the resultant age calculations for the same volcanic rocks under the revised gas cleaning protocol. As shown in Figs. 2 and 7, basaltic rock sample SS06-2 (run ID 564 and 642) shows a dramatic change in the ^{40}Ar signal behavior. The signal variation on one sample aliquot during measurement improved from 244 to 8.5 % with the adoption of the new protocol, so that the derivation of the zero-time signal becomes more reasonable (Table 3). Consequently, the age results become more

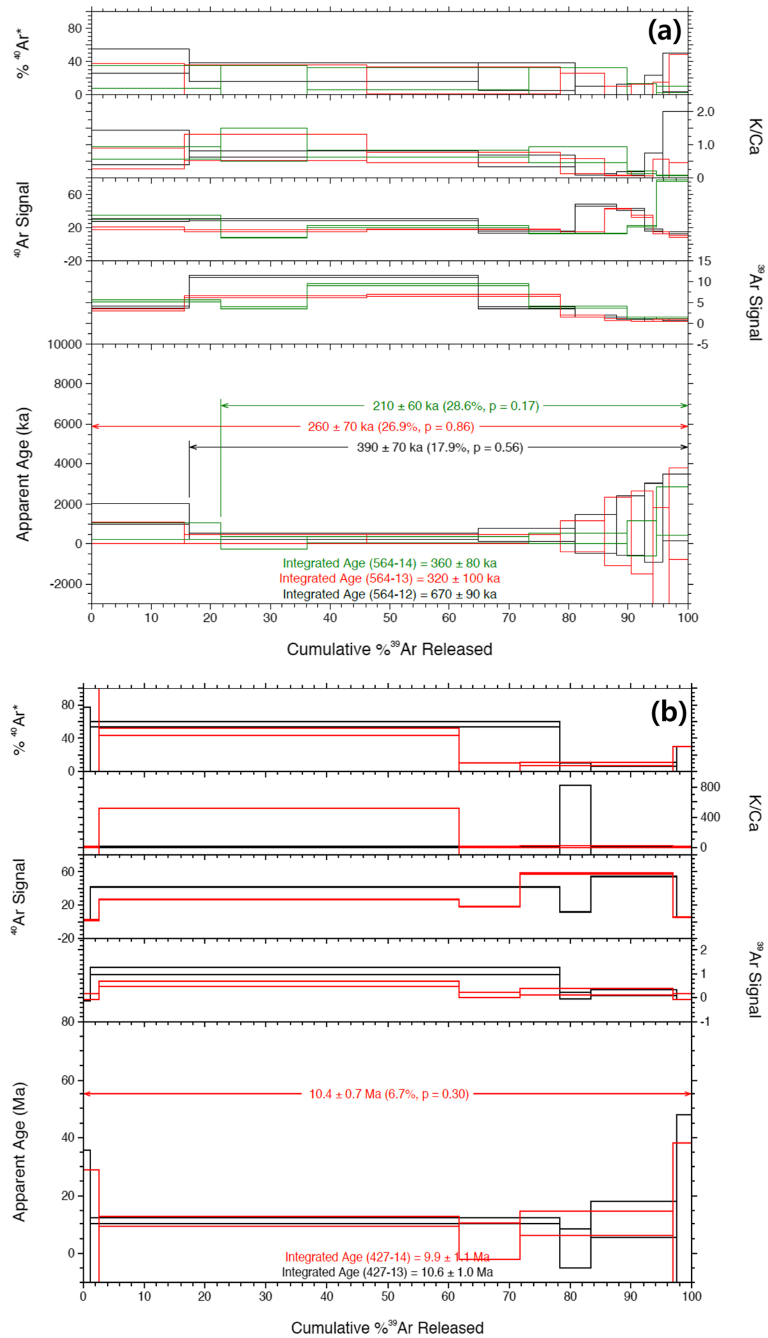

Fig. 3 Age spectra of (**a**) basaltic rock and (**b**) alunite with peak suppression measured under the original sample preparation protocol

precise and geologically compatible from 400 ± 200 Ka to 190 ± 50 Ka (Fig. 4).

The peak suppression effect is also successfully minimized for the sulfur-bearing alunite (Fig. 7). The ^{40}Ar variation during measurement is decreased from 53 to 8.5% and corresponding ages become more precise, from 15 to 1.5% (see Table 2). The precision of the weighted mean age of multiple aliquots improves from 43.1 to 1.4% (Fig. 4 and Table 4).

Application to Quaternary basalt in the Jeongok area, Korea

New ages of 12 basalt samples in the Jeongok area were measured to test the feasibility of the modified gas preparation system. Basaltic volcanism in the Jeongok area, as one of the major Quaternary volcanic episodes in the Korean peninsula, was formed by intraplate magmatism (e.g., Choi et al. 2014). In addition, the mantle source component of the Jeongok

Table 1 Ar isotope analyses of representative aliquots of basaltic rock

Sample ID	Previous protocol						Modified protocol					
	564-06			564-11			642-02			642-06		
	fAmp	±1 sd	% sd	fAmp	± 1 sd	% sd	fAmp	± 1 sd	% sd	fAmp	± 1 sd	% sd
^{40}Ar	67.0140	1.7411	2.6	67.8663	1.1595	1.71	86.1921	0.0603	0.07	116.0573	0.0834	0.07
^{39}Ar	8.5231	0.1577	1.85	9.4345	0.1515	1.61	10.7780	0.0672	0.62	19.9844	0.0997	0.05
^{38}Ar	0.1148	0.1500	130.66	0.1114	0.1744	156.62	0.0126	0.0627	497.12	0.4681	0.0662	14.15
^{37}Ar	2.7807	0.1111	3.99	3.1500	0.1296	4.12	7.6974	0.0599	0.78	10.4150	0.0550	0.53
^{36}Ar	0.1821	0.0078	4.29	0.1978	0.0072	3.62	0.2830	0.0026	0.93	0.3733	0.0035	0.93
Moles (^{40}Ar)	2.22E−15			2.25E−15			2.86E−15			3.85E−15		
%$^{40}Ar^*$	20.8			15.2			4.5			6.9		
Ca/K	2.197			2.301			3.033			2.739		
Age (Ka)	0.82			0.55			0.19			0.21		
± 1 sd	0.17			0.13			0.04			0.03		
% sd	20.37			23.25			20.69			13.41		

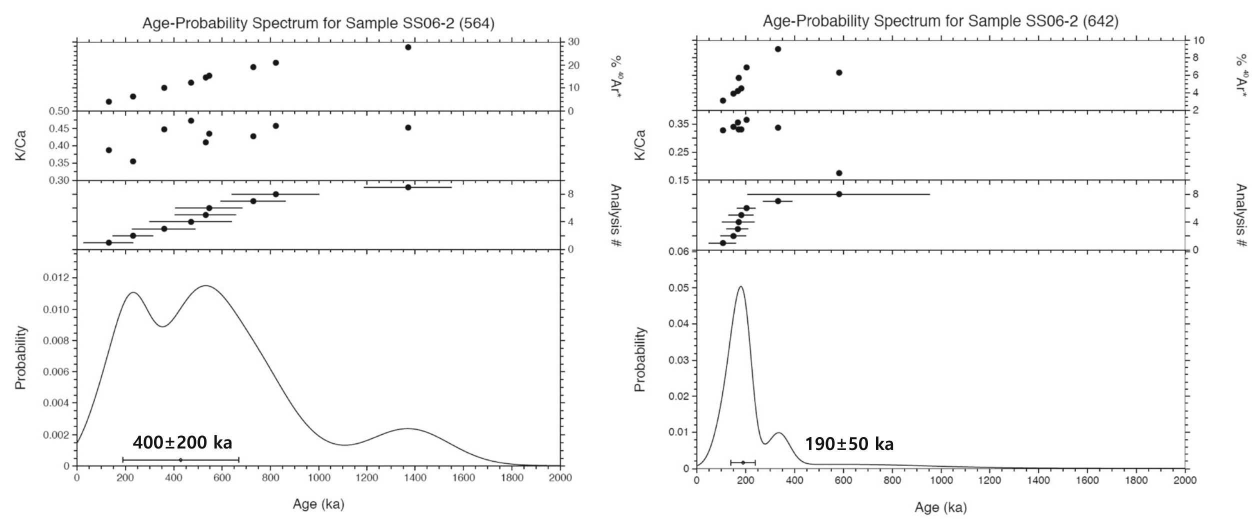

Fig. 4 Age probability diagrams of the basaltic rock. Left and right diagrams represent the $^{40}Ar/^{39}Ar$ ages of multiple aliquots using the original and modified gas preparation protocol, respectively. Note that the the precision of multiple aliquot analysis is significantly improved by using the modified cleaning protocol

basalt is different from that of other Cenozoic basalt in Korea (Choi et al. 2006).

Ryu et al. (2011) suggested that there were two major volcanic eruptions in this area, at ca. 150 and 510 Ka based on K-Ar ages. As K-Ar ages are vulnerable to argon loss, yielding erroneous ages, the step-heated $^{40}Ar/^{39}Ar$ age measurement was adopted to refine the age of volcanic activity in the Jeongok area. Grains of matrix 250-330 μm in size from basaltic rocks were irradiated for an hour using the TRIGA reactor at Oregon State University with Alder Creek sanidine (ACS, 1.193 ± 0.001 Ma: Nomade et al. 2005) as the neutron flux monitor. After irradiation, each sample was stepwise-heated by CO_2 laser and the released gas was cleaned through the newly revised protocol. MassSpec software was used for integration between the laser heating device and mass spectrometer as well as for data reduction.

Representative step-heated $^{40}Ar/^{39}Ar$ age data are shown in Fig. 8 and presented in Table 5. The analyzed samples show a nearly flat age spectrum and well-defined plateau ages. All plateau ages from the analyzed samples are shown in Fig. 9 with the previous K-Ar age data. The revised protocol successfully reproduces $^{40}Ar/^{39}Ar$ age results similar to the average K-Ar ages of 150 ± 10 Ka and 510 ± 10 Ka from Ryu et al. (2011). In addition, other volcanic activity at ca. 270 Ka is prominent, implying that there were more than two volcanic

Table 2 Ar isotope analyses of representative aliquots of alunite

Sample ID	Previous protocol						Modified protocol		
	427-10			427-11				619-12	
	fAmp	± 1 sd	% sd	fAmp	± 1 sd	% sd	fAmp	± 1 sd	% sd
^{40}Ar	104.7595	1.3274	1.27	111.1220	1.5948	1.44	209.5691	0.1125	0.05
^{39}Ar	1.7986	0.2951	16.41	2.9216	0.2942	10.07	4.8741	0.0706	1.45
^{38}Ar	0.0952	0.1101	115.68	0.1788	0.1071	59.89	0.0869	0.0658	75.76
^{37}Ar	0.0481	0.0763	158.68	0.0304	0.0756	249.11	− 0.0705	0.0565	− 80.1
^{36}Ar	0.2541	0.0090	3.55	0.2423	0.0092	3.78	0.2232	0.0027	1.22
Moles (^{40}Ar)	3.48E-15			3.69E-15			6.96E-15		
%^{40}Ar*	28.3			35.6			68.5		
Ca/K	0.209			0.081			− 0.083		
Age (Ma)	8.60			7.07			15.21		
± 1 sd	1.30			0.73			0.23		
% sd			15.12	10.32			1.48		

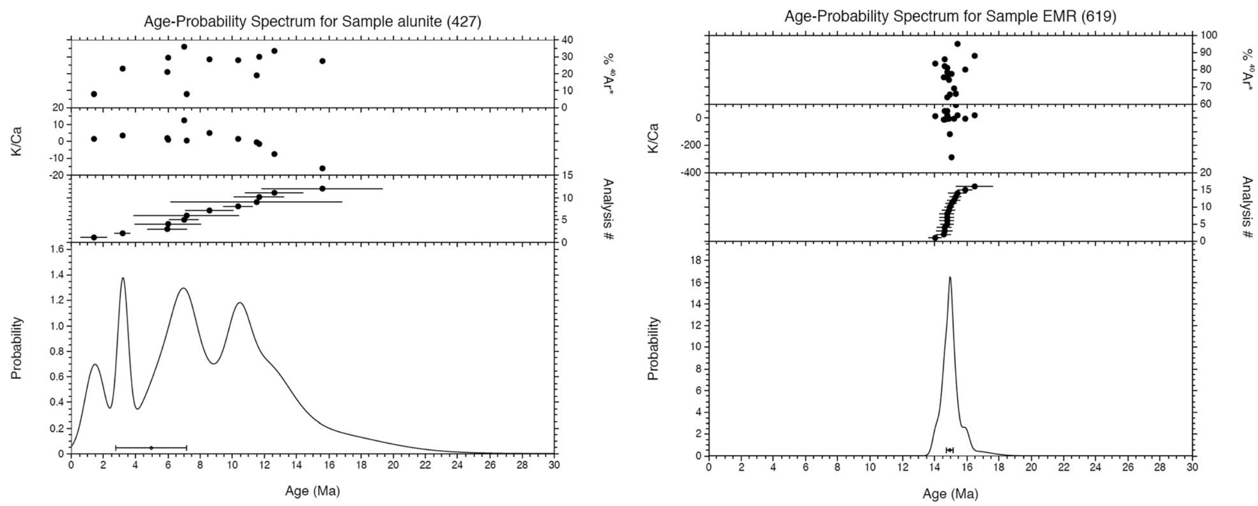

Fig. 5 Age probability diagrams of the alunite sample. Left and right diagrams represent the $^{40}Ar/^{39}Ar$ ages of multiple aliquots using the original and modified gas preparation protocol, respectively.

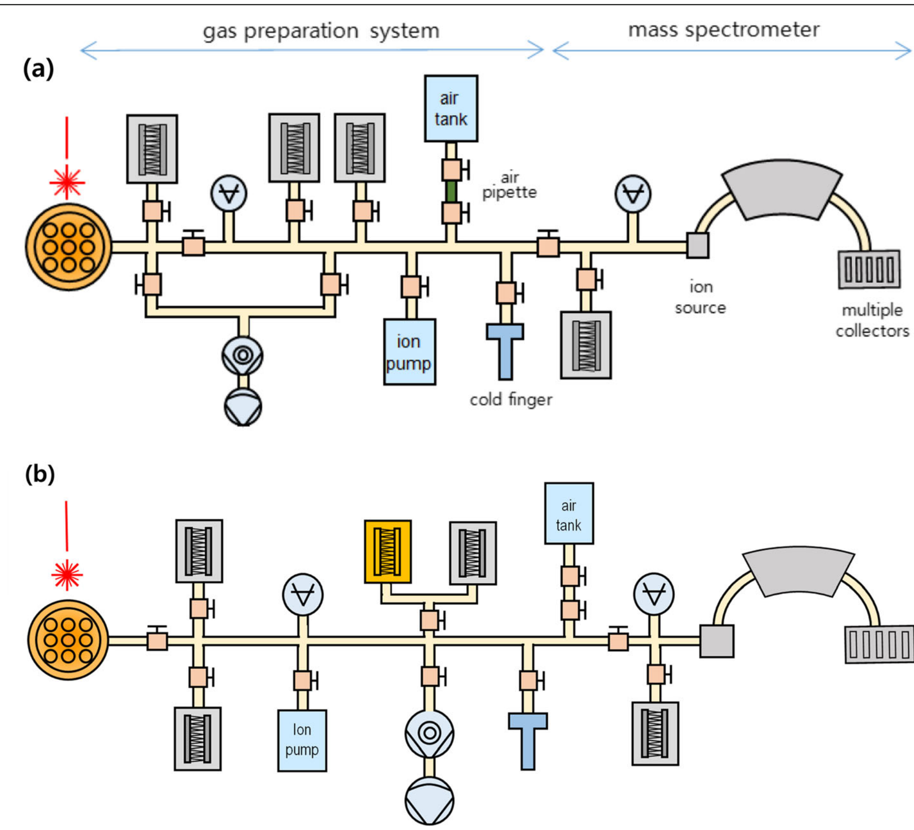

Fig. 6 Schematic diagrams of the Argus VI system at KBSI. Original (**a**) and modified configuration (**b**) of the gas preparation system. Note that one of the getters operates in hot mode

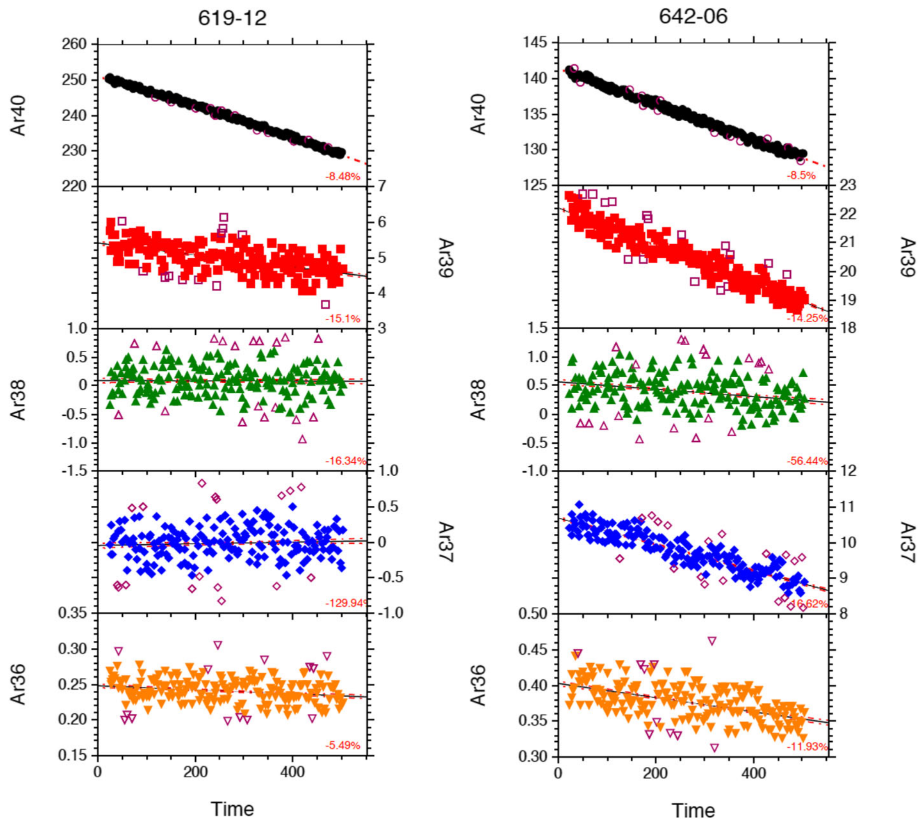

Fig. 7 Examples showing the elimination of the peak suppression effect: (left) alunite, (right) basaltic rock. Note that the intensities of the ^{40}Ar and ^{36}Ar ion beams are decreasing during the measurement

Table 3 Age data for the multiple aliquots of basaltic rock using the modified protocol

	Previous protocol							Modified protocol					
Sample ID	Ca/K	Cl/K	Mol ^{39}Ar ($\times 10^{-15}$)	%^{40}Ar*	Age (Ma)	± 1SD	sample ID	Ca/K	Cl/K	Mol ^{39}Ar ($\times 10^{-15}$)	%^{40}Ar*	Age (Ma)	± 1SD
564-01	2.833	− 0.032	0.042	6.2	0.24	0.07	642-01	2.974	− 0.028	0.036	9.0	0.34	0.04
564-02	2.481	0.119	0.029	101.7	3.07	0.03	642-02	3.033	− 0.046	0.036	4.5	0.19	0.04
564-03	2.632	0.021	0.029	101.5	3.67	0.03	642-03	2.956	− 0.034	0.037	3.9	0.15	0.04
564-04	2.217	− 0.011	0.030	27.4	1.37	0.17	642-04	3.045	− 0.013	0.039	5.6	0.17	0.05
564-05	2.245	− 0.084	0.030	9.9	0.36	0.12	642-05	3.048	− 0.073	0.035	3.0	0.11	0.04
564-06	2.197	− 0.008	0.028	20.8	0.82	0.17	642-06	2.739	0.023	0.066	6.9	0.21	0.03
564-07	2.581	0.013	0.031	3.9	0.14	0.09	642-07	5.791	0.475	0.003	6.3	0.59	0.36
564-08	2.343	− 0.045	0.031	18.8	0.73	0.12	642-08	2.822	0.007	0.074	4.2	0.17	0.03
564-09	2.121	− 0.023	0.030	12.2	0.47	0.16							
564-10	2.448	0.015	0.034	14.3	0.54	0.12							
564-11	2.301	− 0.012	0.031	15.2	0.55	0.13							
			Weighted mean (Ka)		431					Weighted mean (Ka)		191	
			± 1sd		20 (56.2%)					± 1sd		50 (27.5%)	
			MSWD		8.00					MSWD		2.50	

Table 4 Age data for the multiple aliquots of alunite using the modified protocol

Sample ID	Previous protocol						Sample ID	Modified protocol					
	Ca/K	Cl/K	Mol ^{39}Ar (× 10^{-15})	%$^{40}Ar^*$	Age (Ma)	± 1SD		Ca/K	Cl/K	Mol ^{39}Ar (× 10^{-15})	%$^{40}Ar^*$	Age (Ma)	± 1SD
427-01	3.968	− 0.447	0.001	7.8	7.20	3.10	619-01	− 0.126	− 0.051	0.024	63.5	14.83	0.25
427-02	− 1.340	− 1.645	0.001	18.6	11.56	5.10	619-02	0.022	− 0.057	0.013	78.5	14.80	0.29
427-03	1.742	− 0.366	0.001	29.3	6.03	1.90	619-03	0.101	0.199	0.018	83	14.07	0.20
427-04	0.827	0.331	0.004	27.9	10.41	0.69	619-04	− 0.003	− 0.022	0.042	77.4	15.10	0.13
427-05	− 0.062	0.527	0.002	27.1	15.63	3.54	619-05	0.020	− 0.043	0.022	81.8	14.66	0.25
427-06	− 0.126	0.283	0.002	33.4	12.63	1.63	619-06	− 0.067	− 0.017	0.012	85.9	14.64	0.35
427-07	− 0.577	− 0.104	0.002	29.6	11.70	1.34	619-07	− 0.104	− 0.102	0.017	79.9	15.94	0.23
427-08	0.321	0.114	0.016	22.7	3.21	0.33	619-08	0.063	− 0.262	0.005	88	16.51	0.97
427-09	0.701	0.093	0.007	7.9	1.46	0.61	619-09	0.067	0.012	0.010	94.8	15.47	0.34
427-10	0.209	0.041	0.006	28.3	8.60	1.30	619-10	− 0.104	− 0.047	0.021	73.7	14.94	0.21
427-11	0.081	0.097	0.010	35.6	7.07	0.73	619-11	0.069	0.063	0.018	75.1	14.82	0.26
427-12	0.591	0.270	0.006	20.6	5.97	1.08	619-12	− 0.083	− 0.009	0.016	68.5	15.21	0.22
							619-13	0.011	− 0.004	0.019	65.6	15.32	0.19
							619-14	− 0.008	− 0.016	0.054	65.2	14.96	0.10
							619-15	− 0.059	− 0.017	0.016	75.3	14.58	0.28
							619-16	− 0.117	− 0.004	0.018	80.9	14.80	0.24
			Weighted mean (Ma)		5.02				Weighted mean (Ma)			14.97	
			± 1sd		2.0 (43.1%)				± 1sd			0.2 (1.39%)	
			MSWD		18.00				MSWD			3.60	

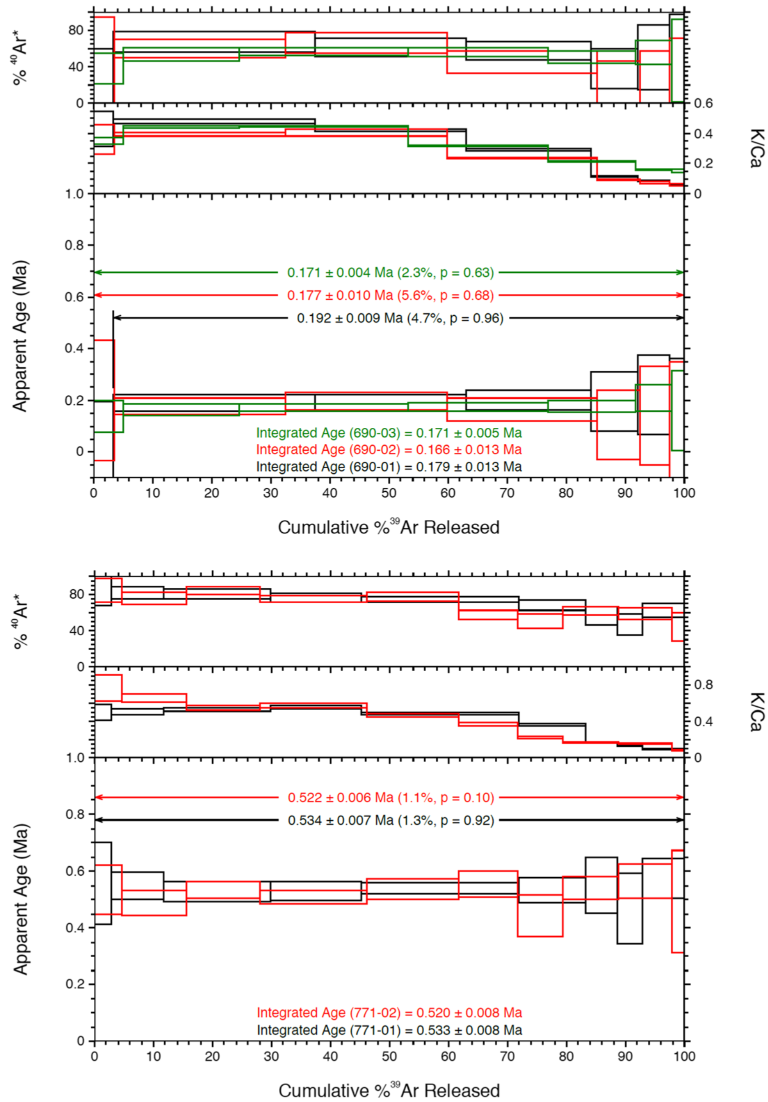

Fig. 8 Age spectra of representative samples of Jeongok basalts

episodes in central Korea. More experiments are currently underway, and the exact timing of multiple volcanic episodes in the Jeongok area will be determined in the future.

Conclusions

The $^{40}Ar/^{39}Ar$ dating protocol for a multi-collector noble gas mass spectrometer and CO_2 laser heating device at KBSI has been modified in order to minimize the peak suppression effect. Operation of one hot getter with three room-temperature getters in the sample preparation system seems to remove the redundant component from the sample effectively and improve the precision of the zero-time isotope signal. This revised technique was applied to Quaternary basaltic rocks in the Jeongok area and successfully reproduced the previous K-Ar age data.

Abbreviations

fAmps: femto Amperes; Ka: Kilo annum; Ma: Mega annum; MSWD: Mean square weighted deviation; TRIGA: Training, Research, Isotope, General Atomics

Acknowledgements

This study was supported by the KBSI grant (C050300). We thank to Dr. Alan Deino in Berkeley Geochronology Center giving the ideas of peak suppression effect. We are also grateful to reviewers who read the manuscripts and gave useful comments.

Authors' contributions

JK conceived of the study and carried out the design of experiment. IJ carried out the sample preparation and the acquisition of data and helped to draft the manuscript. The author(s) read and approved the final manuscript.

Funding

Not applicable.

Table 5 $^{40}Ar/^{39}Ar$ age spectrum data for aliquots of representative samples

	Watt	Ca/K	Cl/K	$^{36}Ar/^{39}Ar$	$\%^{36}Ar(Ca)$	$^{40}Ar^{*}/^{39}Ar$	$Mol^{39}Ar(\times 10^{-16})$	% step	Cum %	$\%^{40}Ar^{*}$	Age (Ka)	± Age
141006-1, Run ID# 689-01 ($J = 0.0002755 \pm 0.0000008$):												
*689-01A	0.3	2.543	0.141	0.00279	12.3	1.0068	0.0076	4.4	4.4	58.2	500	98
*689-01B	0.8	1.810	-0.008	0.00099	24.7	1.0356	0.0709	40.7	45.1	82.5	515	11
*689-01C	1.2	3.183	-0.022	0.00137	31.5	1.0338	0.0396	22.7	67.8	78.9	514	18
*689-01D	1.7	8.023	-0.024	0.00247	44.0	1.1125	0.0166	9.5	77.3	73.1	553	42
*689-01E	2.5	6.900	-0.028	0.00253	36.9	1.0214	0.0283	16.2	93.5	68.4	508	29
*689-01F	3.5	17.215	0.232	0.00417	55.8	1.6478	0.0037	2.1	95.7	75.1	819	218
*689-01G	4.0	13.151	0.039	0.00556	31.9	0.6983	0.0056	3.2	98.9	38.3	347	119
*689-01H	4.7	12.711	0.364	0.02289	7.5	0.2635	0.0020	1.1	100	4	131	342
Integrated Age=											513	13
(*) Plateau Age =											515	9
141006-1, Run ID# 689-02 ($J = 0.0002755 \pm 0.0000008$):												
*689-02A	0.3	2.958	0.247	0.00221	18.1	1.0315	0.0080	4.3	4.3	65.9	513	87
*689-02B	0.8	1.812	0.001	0.00098	25.0	1.0513	0.0823	44.4	48.8	82.9	522	9
*689-02C	1.2	2.614	− 0.024	0.00122	29.0	1.0565	0.0368	19.9	68.7	80.5	525	19
*689-02D	1.7	5.688	0.009	0.00206	37.4	1.0581	0.0389	21	89.7	73.5	526	24
*689-02E	2.5	12.085	− 0.159	0.00452	36.1	1.0797	0.0097	5.3	94.9	55.7	537	74
*689-02F	3.5	12.451	0.003	0.00506	33.2	1.2264	0.0053	2.9	97.8	55	609	132
*689-02G	4.0	13.229	0.065	0.00546	32.8	1.2411	0.0040	2.2	100	53.2	617	181
Integrated Age =											528	12
(*) Plateau Age =											524	8
141006-1, Run ID# 689-03 ($J = 0.0002755 \pm 0.0000008$):												
689-03A	0.3	5.559	0.993	0.00712	10.5	1.0134	0.0025	0.5	0.5	35.1	504	249
689-03B	0.6	2.323	0.031	0.00285	11.0	0.8972	0.0401	8.5	8.5	54.5	446	18
*689-03C	1.1	1.699	− 0.028	0.00123	18.7	1.0487	0.1118	23.8	32.3	78	521	7
*689-03D	1.7	2.356	− 0.003	0.00147	21.6	1.0626	0.1462	31.1	63.5	75.7	528	6
*689-03E	2.5	4.685	0.000	0.00197	32.2	1.0509	0.0828	17.6	81.1	72.7	522	11
*689-03F	3.5	6.940	0.004	0.00251	37.4	1.0204	0.0645	13.7	94.8	68.7	507	13
*689-03G	4.0	9.741	− 0.128	0.00335	39.3	1.1082	0.0142	3	97.8	64.7	551	48
*689-03H	4.6	14.580	0.095	0.00432	45.6	1.0931	0.0103	2.2	100	61	543	68
Integrated Age =											516	5
(*) Plateau Age =											523	4

Table 5 $^{40}Ar/^{39}Ar$ age spectrum data for aliquots of representative samples *(Continued)*

	Watt	Ca/K	Cl/K	$^{36}Ar/^{39}Ar$	$\%^{36}Ar(Ca)$	$^{40}Ar^{*}/^{39}Ar$	$Mol^{39}Ar(\times 10^{-16})$	% step	Cum %	$\%^{40}Ar^{*}$	Age (Ka)	± Age
141006-2A, Run ID# 690-01 (*J* = 0.000273 ± 0.0000008):												
690-01A	0.3	2.342	0.150	0.00351	9.0	-0.2883	0.0056	3.3	3.3	-44	-142	167
*690-01B	0.8	2.100	0.003	0.00093	30.6	0.3848	0.0586	34.2	37.5	66.9	190	16
*690-01C	1.2	2.407	0.011	0.00116	28.1	0.3814	0.0437	25.6	63.1	60.8	188	15
*690-01D	1.7	3.471	0.049	0.00151	31.1	0.4060	0.0364	21.3	84.4	57	200	18
*690-01E	2.5	8.860	− 0.013	0.00341	35.1	0.3906	0.0134	7.9	92.2	37.3	192	56
*690-01F	3.5	11.886	0.132	0.00309	52.0	0.4437	0.0094	5.5	97.7	50.2	219	77
*690-01G	4.0	16.954	− 0.050	0.00434	52.8	0.1473	0.0040	2.3	100	19.4	73	145
690-01H	4.7	17.297	− 1.371	0.00510	45.9	− 0.0825	0.0013	0.8	100	− 10.9	− 41	422
Integrated Age =											179	13
(*) Plateau Age =								96.7			192	9
141006-2A, Run ID# 690-02 (*J* = 0.000273 ± 0.0000008):												
*690-02A	0.3	2.832	0.074	0.00215	17.8	0.4007	0.0055	3.6	3.6	43.5	197	116
*690-02B	0.8	2.563	0.002	0.00117	29.5	0.3555	0.0439	29	32.6	59.3	175	15
*690-02C	1.2	2.487	− 0.020	0.00104	32.2	0.3950	0.0414	27.3	59.9	65.4	195	17
*690-02D	1.7	4.289	0.014	0.00197	29.4	0.3286	0.0385	25.4	85.3	44.4	162	23
*690-02E	2.5	11.130	− 0.290	0.00440	34.2	0.2072	0.0112	7.4	92.6	19.3	102	68
*690-02F	3.5	14.029	− 0.306	0.00489	38.8	0.2804	0.0076	5	97.6	23.9	138	96
*690-02G	4.0	17.476	− 0.552	0.00561	42.1	0.0155	0.0036	2.4	100	1.6	8	169
690-02H	4.7	13.973	− 0.789	0.00401	47.1	− 0.3665	0.0014	0.9	100	− 133.7	− 181	423
Integrated Age =											166	13
(*) Plateau Age =								100			177	10
141006-2A, Run ID# 690-03 (J = 0.000273 ± 0.0000008):												
*690-03A	0.6	2.866	0.027	0.00196	19.8	0.2779	0.0233	5.2	5.2	37.4	137	31
*690-03B	1.1	2.271	− 0.002	0.00128	23.9	0.3312	0.0882	19.6	24.7	53.4	163	11
*690-03C	1.7	2.263	− 0.005	0.00121	25.4	0.3457	0.1287	28.6	53.3	56.5	170	6
*690-03D	2.5	3.164	0.006	0.00137	31.2	0.3530	0.1065	23.6	77	55.9	174	8
*690-03E	3.5	4.796	− 0.063	0.00182	35.5	0.3560	0.0668	14.8	91.8	50.5	175	12
*690-03F	4.0	6.393	0.012	0.00204	42.3	0.4261	0.0281	6.2	98	54.9	210	25
*690-03G	4.6	6.719	0.132	0.00215	42.2	0.3207	0.0090	2	100	46.7	158	77
Integrated. Age =											171	5
(*) Plateau Age =								100			171	4

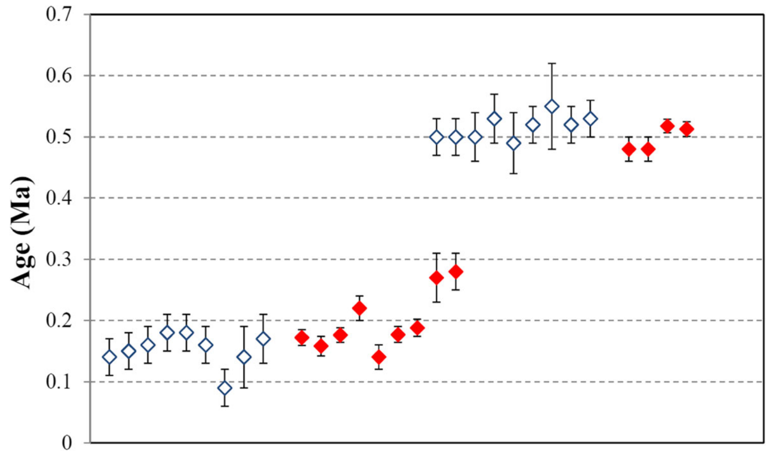

Fig. 9 Summary of age results of Jeongok basalt. Symbols: open diamonds, K-Ar ages from Ryu et al. (2011); closed diamonds, $^{40}Ar/^{39}Ar$ ages of this study. Error bar represents 1σ uncertainties

Availability of data and materials
The datasets used and/or analyzed during the current study are available from the corresponding author on reasonable request.

Competing interests
The authors declare that they have no competing interests.

Received: 28 May 2019 Accepted: 10 February 2020
Published online: 20 February 2020

References
Choi HO, Choi SH, Yu Y. Isotope geochemistry of Jeongok basalts, northernmost South Korea: Implications for the enriched mantle end-member component. J Asian Earth Sci. 2014;91:56–68.
Choi SH, Mukasa SB, Kwon S-T, Andronikov AV. Sr, Nd, Pb and Hf isotopic compositions of late Cenozoic alkali basalts in South Korea: evidence for mixing between the two dominant asthenospheric mantle domains beneath East Asia. Chem Geol. 2006;232:134–51.
Kim J, Choi JH, Jeon SI, Park UJ, Nam SS. ^{40}Ar-^{39}Ar age determination for the Quaternary basaltic rocks in Jeongok Area. J Petrol Soc Korea. 2014; 23:385–91.
Kim J, Jeon SI. $^{40}Ar/^{39}Ar$ age determination using ARGUS VI multiple-collector noble gas mass spectrometer: performance and its application to geosciences. J Anal Sci Tech. 2015;6:4.
McDougall I, Harrison TM. Geochronology and Thermochronology by the $^{40}Ar/^{39}Ar$ method. 2nd ed. New York: Oxford Univ. Press; 1999.
Nomade S, Renne PR, Vogel N, Deino AL, Sharp WD, Becker TA, Jaouni AR, Mundil R. Alder Creek sanidine (ACs-2): A Quaternary $^{40}Ar/^{39}Ar$ dating standard tied to the Cobb Mountain geomagnetic event. Chem Geol. 2005; 218:315–38.
Ryu S, Oka M, Yagi K, Sakuyama T, Itaya T. K-Ar ages of the Quaternary basalts in the Jeongok area, the central part of Korean Peninsula. Geosci J. 2011;15:1–8.

Publisher's Note
Springer Nature remains neutral with regard to jurisdictional claims in published maps and institutional affiliations.